J|A|C|S
ARTICLES
Published on Web 01/21/2003

Ordered Polyelectrolyte Multilayers. Rules Governing Layering in Organic Binary Multilayers

Xavier Arys,[†] Peter Fischer,[‡,§] Alain M. Jonas,*[,†] Marc M. Koetse,[‡,||] André Laschewsky,*[,‡,⊥] Roger Legras,[†] and Erik Wischerhoff[‡,#]

Contribution from the Unité de physique et de chimie des hauts polymères and Unité de chimie des matériaux, Université catholique de Louvain, Place Croix du Sud, 1, B-1348 Louvain-la-Neuve, Belgium

Received September 3, 2002; E-mail: jonas@poly.ucl.ac.be; andre.laschewsky@iap.fhg.de

Abstract: We study the growth and internal structure of polyelectrolyte multilayers obtained by combining three polyanions with nine polycations of the ionene family, of systematically varied chemical architecture. We find that, contrary to a generally held belief, ordered organic multilayers are by no way exceptional, provided one of the polyelectrolytes bears groups which induce structure in water, such as long hydrophobic segments or mesogenic groups. However, this condition is not sufficient, as order will or will not emerge in the multilayer depending on the specific pairing of the polyelectrolytes. The results support the notion that layering in the multilayer results from some degree of prestructuring of a water-swollen layer adsorbed during each step of deposition. These findings pave the way to new possible uses of polyelectrolyte multilayers, for example, for applications requiring preferential alignment or strong confinement of specific functional groups.

Introduction

Electrostatic self-assembly (ESA) of polyelectrolytes (also referred to as layer-by-layer assembly, LBL) is a powerful technique enabling the fabrication of thin organic functional films with nanoscale control over the film structure.[1−7] The versatility and deceptive simplicity of the assembly process, which consists of the sequential adsorption of polyions of opposite charges (with rinsing and drying steps being applied between), resulted in a growing interest for this method over the last 10 years. However, in contrast with naive cartoons sometimes encountered in the literature, the internal structure of most organic binary $(A/B)_n$ ESA films was shown to be highly disordered: Successively adsorbed layers of polyelectrolytes interpenetrate so strongly that the compositional fluctuation perpendicular to the surface is completely smoothed out.[4] Although stratified in the sense that the location of a chain is directly related to the step at which it was deposited in the succession of adsorption events,[4,8] most organic $(A/B)_n$ films should be considered as molecular-level blends of polyelectrolytes.[9,10] Consistently, no Bragg reflection due to layering appears in X-ray or even neutron reflectograms of such films,[11−13] even though Bragg reflections are observed for more complex purely organic systems of the $\{(A/B)_m/(C/D)_p\}_n$-type,[4,14−17] or for hybrid binary $(A/B)_n$ systems made of rigid inorganic platelets combined with an organic polyion.[18−22] The lack of true layering in ESA films may be a limitation of the technique, because well-organized multilayers are required for

[†] Unité de physique et de chimie des hauts polymères.
[‡] Unité de chimie des matériaux.
[§] Present address: Bayer AG; KU-FE/PCS; Rheinuferstrasse 7-9; D-47829 Krefeld; Germany.
[||] Present address: Macromolecular and Organic Chemistry, Eindhoven University of Technology, The Netherlands.
[⊥] Present address: Fraunhofer Institut für Angewandte Polymerforschung FhG-IAP; Geiselbergstrasse 69; D-14476 Golm; Germany.
[#] Present address: Glaucus Proteomics B.V.; P.O. Box 54; NL-3980 CB Bunnik; The Netherlands.

(1) Decher, G.; Hong, J. D. *Ber. Bunsen-Ges. Phys. Chem.* **1991**, *95*, 1430.
(2) Lvov, Y. M.; Decher, G. *Crystallogr. Rep.* **1994**, *39*, 628.
(3) Sano, M.; Lvov, Y.; Kunitake, T. *Annu. Rev. Mater. Sci.* **1996**, *26*, 153.
(4) Decher, G. *Science* **1997**, *277*, 1232.
(5) Decher, G.; Eckle, M.; Schmitt, J.; Struth, B. *Curr. Opin. Colloid Interface Sci.* **1998**, *3*, 32.
(6) Arys, X.; Jonas, A. M.; Laschewsky, A.; Legras, R. In *Supramolecular Polymers*; Cifferi, A., Ed.; Marcel Dekker: New York, 2000; p 505.
(7) Bertrand, P.; Jonas, A. M.; Laschewsky, A.; Legras, R. *Macromol. Rapid Commun.* **2000**, *21*, 319.
(8) Joly, S.; Kane, R.; Radzilowski, L.; Wang, T.; Wu, A.; Cohen, R. E.; Thomas, E. L.; Rubner, M. F. *Langmuir* **2000**, *16*, 1354.
(9) Wu, A.; Yoo, D.; Lee, J. K.; Rubner, M. F. *J. Am. Chem. Soc.* **1999**, *121*, 4883.
(10) Schlenoff, J. B.; Ly, H.; Li, M. *J. Am. Chem. Soc.* **1998**, *120*, 7626.
(11) Korneev, D.; Lvov, Y.; Decher, G.; Schmitt, J.; Yaradaikin, S. *Physica* **1995**, *B213 & 214*, 954.
(12) Kellogg, G. J.; Mayes, A. M.; Stockton, W. B.; Ferreira, M.; Rubner, M. F.; Satija, S. K. *Langmuir* **1996**, *12*, 5109.
(13) Lösche, M.; Schmitt, J.; Decher, G.; Bouwman, W. G.; Kjaer, K. *Macromolecules* **1998**, *31*, 8893.
(14) Decher, G.; Lvov, Y.; Schmitt, J. *Thin Solid Films* **1994**, *244*, 772.
(15) Schmitt, J.; Grünewald, T.; Decher, G.; Pershan, P. S.; Kjaer, K.; Lösche, M. *Macromolecules* **1993**, *26*, 7058.
(16) Tarabia, M.; Hong, H.; Davidov, D.; Kirstein, S.; Steitz, R.; Neumann, R.; Avny, Y. *J. Appl. Phys.* **1998**, *83*, 725.
(17) Hong, H.; Steitz, R.; Kirstein, S.; Davidov, D. *Adv. Mater.* **1998**, *10*, 1104.
(18) (a) Kleinfeld, E. R.; Fergusson, G. S. *Science* **1994**, *265*, 370. (b) *Chem. Mater.* **1995**, *7*, 2327. (c) *Chem. Mater.* **1996**, *8*, 1575.
(19) (a) Kotov, N. A.; Dékány, I.; Fendler, J. H. *J. Phys. Chem.* **1995**, *99*, 13065. (b) Kotov, N. A.; Haraszti, T.; Turi, L.; Zaval, G.; Geer, R. E.; Dékány, I.; Fendler, J. H. *J. Am. Chem. Soc.* **1997**, *119*, 6821.
(20) Kaschak, D. M.; Mallouk, T. E. *J. Am. Chem. Soc.* **1996**, *118*, 4222.
(21) (a) Sasaki, T.; Ebina, Y.; Watanabe, M.; Decher, G. *Chem. Commun.* **2000**, *21*, 2163. (b) Sasaki, T.; Ebina, Y.; Tanaka, T.; Watanabe, M.; Decher, G. *Chem. Mater.* **2001**, *13*, 4661.
(22) (a) Glinel, K.; Laschewsky, A.; Jonas, A. M. *Macromolecules* **2001**, *34*, 5267. (b) Glinel, K.; Laschewsky, A.; Jonas, A. M. *Langmuir* **2002**, *18*, 1408. (c) Vuillaume, P. Y.; Jonas, A. M.; Laschewsky, A. *Macromolecules* **2002**, *35*, 5004. (d) Glinel, K.; Laschewsky, A.; Jonas, A. M. *J. Phys. Chem. B* **2002**, *106*, 11246.

a number of applications requiring the precise placement of active functional groups in confined layers.

Recently, organic $(A/B)_n$ films were reported, exhibiting true layering as judged from the presence of Bragg peaks in X-ray reflectograms.[23,24] These films were based on an ionene capable of forming a lyotropic mesophase. The intrinsic drive of this unique polyelectrolyte to microphase-separate or to self-organize in water was considered to be responsible for the formation of an ordered film structure extending over long distances. It was also shown that the resulting layering does not strictly coincide with the sequence of adsorption events, more than one stratum being deposited per dipping cycle.[23] In the present paper, we present a much larger ensemble of results obtained on a set of ionenes of systematically varied chemical architecture, aimed at unraveling the relationships between the internal structure of binary $(A/B)_n$ ESA films and of related bulk complexes, and the chemical structure and physicochemical properties of the polyelectrolytes. We show that truly layered films displaying Bragg peaks can be obtained, provided polyelectrolytes be properly designed, and we extract general rules governing structure formation in binary ESA films, mainly using X-ray scattering techniques.

Experimental Section

Materials. (a) Polyelectrolytes. The polyelectrolytes used in this study are presented in Figure 1. The synthesis and characterization of the polycations were reported elsewhere (**1**, ref 25; **2**, **5**, **7**, **8**, ref 26; **3**, **4**, ref 27; **6**, ref 28; **9**, ref 29). From ^{1}H nuclear magnetic resonance, the degrees of polymerization of most polycations are known to be above at least 20,[25,26] although very high molar masses are not probable given the general properties of ionenes.[30] Poly(vinyl sulfate) (**PVS**), poly(vinyl sulfonate) (**PVSO**), and poly(styrene sulfonate) (**PSS**) were purchased from Aldrich and used without purification.

(b) Substrates. One-side polished n-type (100) silicon substrates were purchased from ACM (France) and cut to get rectangles of 3 cm $\times$ 1 cm. Substrates were cleaned by immersion for 20 min in a hot 1:1 vol 98% H_2SO_4:27% H_2O_2 mixture ("piranha solution"; caution, piranha reacts violently with organic compounds and should not be stored in closed containers), followed by extensive rinsing with ultrapure water (obtained by deionization and purification using the MilliQ system from Millipore).

(c) Multilayer Buildup. Substrates were dipped in a polycation solution for 10 min (unless otherwise specified), rinsed thrice by immersion in ultrapure water (3 $\times$ 1 min), and then dipped for 10 min in a polyanion solution and rinsed thrice. This deposition procedure was then cycled to obtain multilayers. The samples were air-dried only at the end of their fabrication. The pH of all polyelectrolyte solutions was adjusted to 1 with hydrochloric acid. Unless otherwise stated, polycation and polyanion solutions were 2×10^{-2} M in monomer charge (assuming protonation of the 4-(pyridine-3yl azo)-phenyl side group for polycations **2**, **5**, and **8**). All solutions were prepared from ultrapure water and were used within 48 h. For each pair of polyelectrolytes studied, the growth of multilayers was monitored on a set of samples, synthesized under strictly identical conditions except for the number of dipping cycles (parallel dipping of a set of substrates).

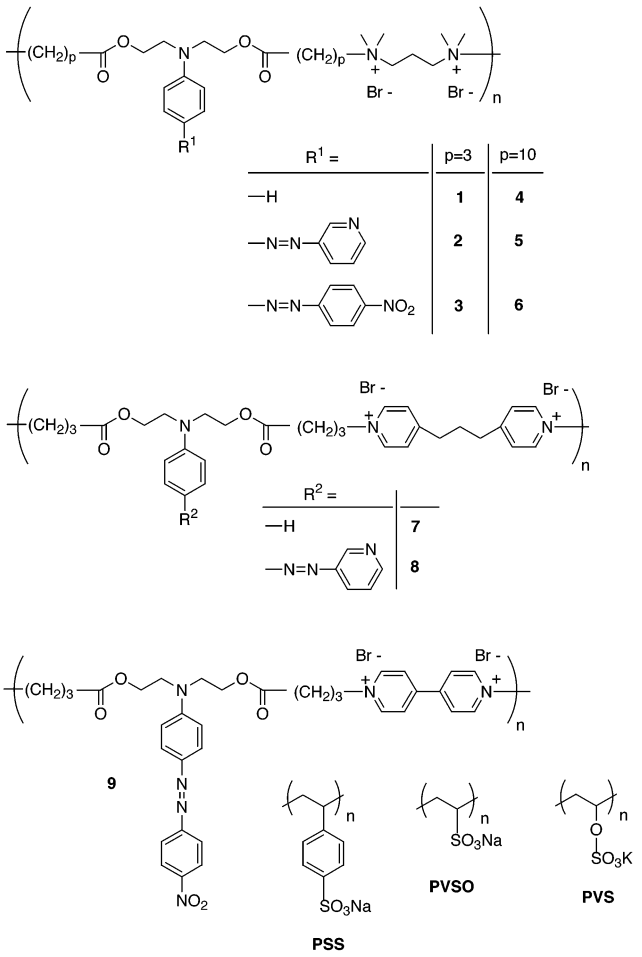

Figure 1. Chemical structures of the polyelectrolytes used in this study.

(d) Polyelectrolyte Complexes. Bulk polyelectrolyte complexes were obtained by mixing under vigorous stirring the polycation and polyanion solutions used for the preparation of the polyelectrolyte multilayers. After being decanted, the solutions were filtered, and the complexes were collected and dried in air.

Methods. (a) Small-Angle X-ray Scattering (SAXS). SAXS was performed to obtain the long-range structure of bulk complexes and dry polyelectrolytes. SAXS was measured in transmission in an evacuated Kratky compact camera mounted on a Siemens rotating anode (Ni-filtered Cu Kα radiation, 40 kV/300 mA). A calibrated position-sensitive proportional counter (mBraun, Garching, Germany) was used to record the scattering patterns.

(b) Wide-Angle X-ray Scattering (WAXS). The experimental setup is based on a Siemens D5000 2-circles goniometer. X-rays of 1.5418 Å wavelength (Cu Kα) were obtained from a rotating anode. Monochromatization was achieved with the help of a secondary graphite monochromator, complemented with pulse height discrimination (scintillation counter). Soller slits placed in the incident and reflected beams limited axial divergence to 0.02°. Powder samples were deposited on silicon single crystals (cut parallel to {510}). Measurements were performed in reflection in an asymmetrical mode. The incoming angle of the X-ray beam on the silicon substrate was held fixed at 6°.

(c) X-ray Reflectometry (XRR). The same goniometer used for WAXS studies was used for XRR. Proper collimation of the beam was obtained by using slits adjustable with micrometer precision. The vertical divergence of the incoming beam was typically 0.0084°. The

(23) Arys, A.; Laschewsky, A.; Jonas, A. M. *Macromolecules* **2001**, *34*, 3318.
(24) Glinel, K.; Jonas, A. M.; Laschewsky, A.; Vuillaume, P. Y. In *Thin Films: Polyelectrolyte Multilayers and Related Multicomposites*; Decher, G., Schlenoff, J. B., Eds.; Wiley-VCH: New York, in press.
(25) Koetse, M.; Laschewsky, A.; Mayer, B.; Rolland, O.; Wischerhoff, E. *Macromolecules* **1998**, *31*, 9316.
(26) Fischer, P.; Laschewsky, A.; Wischerhoff, E.; Arys, X.; Jonas, A.; Legras, R. *Macromol. Symp.* **1999**, *137*, 1.
(27) Charlier, V.; Laschewsky, A.; Mayer, B.; Wischerhoff, E. *Macromol. Symp.* **1997**, *126*, 105.
(28) Koetse, M.; Laschewsky, A.; Jonas, A. M.; Verbiest, T. *Colloids Surf., A: Physicochem. Eng. Aspects* **2002**, *198*, 275.
(29) Laschewsky, A.; Wischerhoff, E.; Kauranen, M.; Persoons, A. *Macromolecules* **1997**, *30*, 8304.
(30) Meyer, W. H.; Dominguez, L. In *Polymer Electrolyte Review*; McCallum, J. R., Vincent, C. A., Eds.; Elsevier Applied Science: London, 1990; Vol. 2, pp 191−228.

vertical acceptance of the detector was fixed by a 200 μm wide slit placed at 20 cm distance from the sample. A special automated alignment procedure allowed one to position the sample within a few micrometers from the goniometer center. More information on this setup can be found elsewhere.[31] XRR data were scaled to unit incident intensity and corrected for spill-over. The data are reported as a function of k_{z0}, the component perpendicular to the interface of the wavevector in a vacuum of the incident photons (i.e., $k_{z0} = (2\pi/\lambda) \sin \theta$, where λ is the X-ray wavelength, and θ is one-half of the angle between the incident and reflected beams).

To obtain a view of the data in direct space, a normalized Patterson function $P(r)$ was computed from reflectivity using:[32]

$$P(r) = \frac{1}{2\pi} \int_{-\infty}^{\infty} \frac{R(k_{z1})}{R_F(k_{z1})} e^{2ik_{z1}r} \, dk_{z1} \quad (1)$$

where k_{z1} is the component perpendicular to the interface of the wavevector *in the film*, and $R_F(k_{z1})$ is the Fresnel reflectivity of the bare and perfectly smooth substrate computed at k_{z1}. In the frame of the first Born approximation, that is, kinematical theory, this function can be shown to be equal to the auto-correlation of the electron density gradient:[33]

$$P(r) = \frac{1}{\rho_s^2} \int_{-\infty}^{\infty} \frac{d\rho(z)}{dz} \frac{d\rho(z+r)}{dz} \, dz \quad (2)$$

where ρ_s is the electron density of the substrate, and $\rho(z)$ is the electron density in the film at z, laterally averaged over the coherence area of the photons. The thickness of the samples was defined as the location corresponding to the maximum of the final peak in $P(r)$, originating from correlation between the film/air and substrate/film interfaces.

For a few selected samples, electron density profiles were obtained from the X-ray reflectivity data, using a modified version of a method originally proposed by Singh et al.[34] The electron density profile perpendicular to the film surface was expressed as the sum of two terms:

$$\rho_{el}(z) = \langle \rho_1(z) \rangle + \rho_2(z) \quad (3)$$

The first term, $\langle \rho_1(z) \rangle$, describes the average shape of the electron density profile. It was written as

$$\langle \rho_1(z) \rangle = \rho_s + (\rho_f - \rho_s) \cdot \zeta\left(\frac{z}{\sigma_s}\right) - \rho_f \cdot \zeta\left(\frac{z-d}{\sigma_f}\right) \quad (4)$$

where $\zeta(x) = 1/2(1 + \mathrm{erf}(x/\sqrt{2}))$, ρ_s is the electron density of the substrate, ρ_f is the average electron density of the film, d is the thickness of the film, and σ_s and σ_f are the root-mean-square roughness of the substrate and of the film, respectively.[35] The second term in eq 3, $\rho_2(z)$, was introduced to represent regular modulations of the electron density of the film. It was written as a damped Fourier series:

$$\rho_2(z) = \left(\sum_{n=1}^{m} A_n \cos(2\pi n z/d_{Bragg} - \phi_n)\right) \cdot \exp\left(-\frac{z}{L_{coh}}\right) \cdot \zeta\left(\frac{z}{\sigma_s}\right) \cdot \zeta\left(\frac{z-d}{\sigma_f}\right) \quad (5)$$

into which d_{Bragg} is the repeat period of the internal modulation of the film, and L_{coh} is its coherence length. The multiplication by the ζ functions ensures that the contribution of $\rho_2(z)$ vanishes outside of the film. As shown by Singh et al.,[34] the intensity of the nth Bragg peak is related to the amplitude A_n of the nth Fourier component of the series, whereas the shape of the nth Bragg peak is related to the phase coefficient ϕ_n. In the present work, fits were performed over $0 < k_{z0} < 0.2$ Å^{-1}, into which only the first Bragg peak was observed, if any. Therefore, the Fourier series was limited to its first term ($m = 1$). The profile was then discretized into a large number of slabs of 2.5 Å thickness, and the reflectivity was computed using Parratt's dynamical theory.[36,37] The nine parameters describing the density profile (ρ_s, ρ_f, d, σ_s, σ_f, d_{Bragg}, L_{coh}, A_1, ϕ_1), plus a scaling parameter, were then varied using a Marquardt−Levenberg algorithm,[38] until the model accurately described the experimental data.

(d) Ellipsometry. A Digisel rotating compensator ellipsometer from Jobin−Yvon/Sofie instruments (France), working at 6328 Å (He−Ne laser), was used in this study. To compensate for some systematic errors (imperfections and residual misalignment of the optical components), measurements were carried out with the analyzer at +45° and −45° (with respect to the plane of incidence).[39] A model consisting of an isotropic film on a flat substrate was used to fit the ellipsometric angles.[40] The refractive index of silicon was taken to be 3.881−j0.019.[41] When possible, the effective refractive index of the film was obtained from the ellipsometric measurements by fitting trajectories in the (ψ,Δ) plane corresponding to samples of increasing thickness, neglecting film absorption which is small at the working wavelength of the ellipsometer. Otherwise, the refractive index was arbitrarily set either to the refractive index of the most closely related system (when possible) or to 1.55.

(e) Miscellaneous. The birefringence of the ionenes and their solution in water was studied in transmission between crossed polarizers with an AX70 Olympus optical microscope.

Results

Ionenes. The polycations used in this study are presented in Figure 1. They all belong to the ionene family; that is, they contain quaternary ammonium fragments as part of their repeat units. Different residues were grafted on a common pendent phenyl group, and aliphatic spacers of variable length were included in the main chain. A first set of ionenes (**1**−**6**) serves to probe the effects, on multilayer formation and structure, of the hydrophilic/hydrophobic balance of the backbone and of the bulkiness and mesogenic character of the side group. The 4-(4′-nitrophenylazo)-phenyl side group of ionenes **3**, **6**, and **9** is known to be mesogenic;[42] the 4-(pyridine-3yl azo)-phenyl of ionenes **2**, **5**, and **8** is mesogenic, too, but seems to be a much weaker mesogen.[42] A second set of ionenes (**7**−**9**) allows one to investigate effects related to the rigidity of the backbone and to the accessibility and local distribution of the cationic charge of the polymers.

The solid-state structure of dry ionenes was probed at room temperature by polarized optical microscopy and small- and wide-angle X-ray scattering. In addition, solutions of the ionenes in water were examined between crossed polarizers, to detect the possible presence of lyotropic mesophases. Results are reported in Table 1 (complete diffractograms can be found elsewhere[31]).

(31) Arys, X. Understanding Ordering in Polyelectrolyte Multilayers: Effect of the Chemical Architecture of the Polycation. Ph.D. Dissertation; Université catholique de Louvain, Louvain-la-Neuve, Belgium, 2000.
(32) Bollinne, C.; Stone, V. W.; Carlier, V.; Jonas, A. M. *Macromolecules* **1999**, *32*, 4719.
(33) Pershan, P. S.; Als-Nielsen, J. *Phys. Rev. Lett.* **1984**, *52*, 759.
(34) Singh, N.; Tirrell, M.; Bates, F. S. *J. Appl. Crystallogr.* **1993**, *26*, 650.
(35) For sample (**9**/**PSS**)$_6$, a supplementary ζ function needed to be introduced to properly describe the film.
(36) Parratt, L. G. *Phys. Rev.* **1954**, *95*, 359.
(37) Parratt, L. G. *J. Chem. Phys.* **1956**, *53*, 597.
(38) Press, W. H.; Teukolsky, S. A.; Vetterling, W. T.; Flannery, B. P. *Numerical Recipes in C*, 2nd ed.; Cambridge University Press: Cambridge, 1992.
(39) Kleim, R.; Kuntzler, L.; El Ghemmaz, A. J. *J. Opt. Soc. Am. A* **1994**, *11*, 2550.
(40) Azzam, R. M. A.; Bashara, N. M. *Ellipsometry and Polarized Light*; North-Holland: Amsterdam, 1977.
(41) Aspnes, D. E.; Studna, A. A. *Phys. Rev. B* **1983**, *27*, 985.
(42) Toyne, K. J. In *Thermotropic Liquid Crystals*; Gray, G. W., Ed.; John Wiley & Sons: Chichester, 1987; p 30.

Table 1. Structural Data of Ionenes **1**−**9**, and of Their Complexes Obtained by Coprecipitation with **PVS**, **PVSO**, or **PSS**

ionene	semicrystalline character (solid state)[a]	low-angle spacing (solid state)[b] (Å)	optical birefringence (solid state)	optical birefringence (solutions in water)	structure of bulk complex with **PVS**[d]	structure of bulk complex with **PVSO**[d]	structure of bulk complex with **PSS**[d]
1	no	none	no	no	sol.	sol.	sol.
2	no	none	no	no	am.	−	am.
3	no	none	yes	no	ord. (28 Å)[e]	am.	am.
4	no	31[c]	yes	no	am.	ord. (29 Å)	ord. (30 Å)
5	yes	28[c]	yes	yes	ord. (24 Å)	ord. (24 Å)	am.
6	no	46[c]	yes	no	−	−	am.
7	yes	none	yes	no	sol.	−	−
8	yes	none	yes	no	sol.	−	am.
9	yes	35	yes	yes	am.	am.	am.

[a] As judged from the presence of sharp interferences in the WAXS diffractogram of the compound. [b] Distance corresponding to Bragg peaks in the SAXS range. [c] Two or three reflections were found for this compound, with repeat distances equal to the long spacing divided by the order of the reflection, demonstrating a lamellar supramolecular organization. [d] "sol.", soluble complex; "am.", insoluble complex showing no Bragg reflection by SAXS or WAXS; "ord.", insoluble complex displaying SAXS long spacings (repeat period indicated between parentheses); "−", no data available because of lack of material. [e] The structure of this complex was found to be metastable, as indicated by the disappearance of low-angle reflections upon holding the complex in water.

It is difficult to rationalize the semicrystalline character of the polycations on the basis of their chemical structure, except for the fact that replacing the aliphatic moieties by aromatic ones seems to favor crystallinity. The incorporation of long aliphatic spacers in the backbone of polymers (**4**−**6**) or of the mesogenic 4-(4′-nitrophenylazo)-phenyl side group in aromatic ionenes (**9**) induces some degree of organization in the solid state, as testified by the long spacings detected by SAXS. For ionenes **4**−**6** containing $-(CH_2)_{10}-$ fragments, SAXS indicates the occurrence of a lamellar organization in the solid state, probably due to microphase separation between the hydrophobic spacers and the rest of the molecule. In some instances, the trend to form organized supramolecular structures is partially conserved in water, as testified by ionenes **5** and **9** which display liquid crystallinity in water (lyotropic mesophases).

Bulk Complexes. Polycations **1**−**9** were coprecipitated with polyanions **PSS**, **PVS**, or **PVSO**, to form soluble or insoluble bulk complexes (Table 1). Insoluble complexes were collected by filtration. None of the insoluble complexes were found to be crystalline as judged by WAXS. However, some of them displayed broad low-angle reflections when probed by SAXS (Table 1), suggesting partial organization of the bulk complexes. Excluding from the discussion ionene **3**, which only forms a metastable transient supramolecular organization when complexed with **PVS**, it appears that organized bulk complexes only form for ionenes containing long hydrophobic $(CH_2)_{10}$ sequences. This is a necessary but not a sufficient condition, as ordering may be lost when complexing the polycation with specific polyanions (e.g., **4** gives supramolecularly ordered complexes when combined with **PVSO** or **PSS**, not with **PVS**). Nevertheless, it is obvious that partial phase separation or clustering of long hydrophobic segments in water must be the reason for the formation of organized bulk complexes. Compound **9**, which was shown to form a lyotropic mesophase in water, did not provide organized complexes when combined with **PSS**, but lack of material unfortunately prevented us from checking its behavior when it was coprecipitated with **PVS** or **PVSO**.

Growth of ESA Films. For many pairs of ionenes/polyanions, a set of films was grown on cleaned silicon wafers by the layer-by-layer assembly method, and their thickness was measured by ellipsometry or X-ray reflectometry. For some pairs of polyelectrolytes, a linear (or close to linear) growth was obtained versus the number of dipping cycles (i.e., a complete cycle of adsorption of a polycation and of a polyanion), as indicated in Table 2. Other systems were found to grow linearly over a limited number of dipping cycles, and then to diverge, while others grew in a nonlinear fashion from the very beginning of the deposition process. Some pairs failed to provide films. Increments of thickness per deposition cycles (Δd) most often lie in the range 10−40 Å, but the **3/PVS** and **5/PVS** pairs provide much larger values, in the 100 Å range. It is difficult to fully rationalize the values of Δd on the basis of the molecular architecture of the ionenes only, even though it appears that larger values of Δd tend to be obtained for the ionenes bearing the bulky and mesogenic 4-(4′-nitrophenylazo)-phenyl side group (ionenes **3**, **6**, **9**).

Internal Structure of ESA Films. The internal structure of the films was assessed by X-ray reflectometry. Figure 2 provides selected X-ray reflectograms for the pairs of polyelectrolytes tested. Most reflectograms display regular oscillations, which are damped with increasing angle. These so-called Kiessig fringes originate from constructive interference between waves scattered at the film/air and substrate/film interfaces, allowing one to easily determine the thickness of the film. In addition, additional positive/negative peaks show up for some pairs of polyelectrolytes, due to constructive/destructive interference from waves scattered at regularly spaced inner interfaces (Bragg reflections).

These data can be more easily analyzed in direct space, by computing Patterson functions, $P(r)$, from the reflectograms (Figure 3). Within the first Born approximation, $P(r)$ is proportional to the probability of finding in a film two interfaces separated by a distance r, positive peaks being related to interfaces having electron density gradients of identical sign, and negative peaks being related to interfaces of opposite gradient.[33] The Patterson functions display a broad terminal peak, due to correlation between the substrate/film and film/air interfaces, which is the translation in direct space of the Kiessig fringes mentioned previously. For some systems, this peak is absent due to extreme roughness of the film/air interface, in which case Kiessig fringes also vanish in the reflectograms. In addition, regularly spaced interfaces within the film show up as regular oscillations in $P(r)$. The amplitudes of these oscillations are related to the sharpness and regularity of the inner contrast of electron density, while their spatial extent provides a direct view of the coherence of the stacking.

The values of the repeat period between inner interfaces are reported in Table 2. In this table, the films have been sorted

Table 2. Structural Data (Mode of Growth, Increment of Thickness per Deposition Cycle, Internal Structure, Internal Repeat Periods) of **LBL** Films Grown by Combining Ionenes **1**−**9** with **PVS**, **PVSO**, or **PSS**

ionene	mode of growth when combined with **PVS**[a]	mode of growth when combined with **PVSO**[a]	mode of growth when combined with **PSS**[a]	internal organization when combined with **PVS**[b]	internal organization when combined with **PVSO**[b]	internal organization when combined with **PSS**[b]
1	part. linear ($\Delta d = 10.9$ Å, $0 < n < 13$)	no growth	not linear	no order	not applic.	no order
2	part. linear ($\Delta d = 12.4$ Å, $0 < n < 7$)	part. linear ($\Delta d = 9$ Å, $0 < n < 6$)	part. linear ($\Delta d = 13.5$ Å, $0 < n < 7$)	no order	no order	no order
3	linear ($\Delta d = 118$ Å)	−	−	part. ord. (23.8 Å)	−	no order [ref 26]
4	linear ($\Delta d = 27.9$ Å)	not linear	not linear	part. ord. (33.5 Å)	no order	part. ord. (28.8 Å)
5	linear ($\Delta d = 88$ Å)	film growth	linear ($\Delta d = 21.9$ Å)	ordered (23.8 Å)	ordered (24.0 Å)	no order
6	film growth	−	linear ($\Delta d = 38.4$ Å)	part. ord.?	−	part. ord. (18.3 Å)
7	linear ($\Delta d = 9.8$ Å)	−	−	no order	−	−
8	no growth	−	linear [ref 26]	not applic.	−	−
9	linear ($\Delta d = 27.7$ Å)	not linear	linear ($\Delta d = 39$ Å)	part. ord. (very weak) (26.0 Å)	ordered (23.3 Å)	no order

[a] Mode of growth: "linear", linear increase of thickness with number of dipping cycles (increment per cycle, Δd, given between parentheses); "part. linear", linear growth over a restricted number of dipping cycles n (increment and range of n given between parentheses); "not linear", nonlinear growth from the onset; "no growth", no film could be grown with this pair of polyelectrolytes; "film growth", film formation was checked, but the available data are too scarce to classify the mode of growth; "−", no data acquired for this pair of polyelectrolytes. [b] Internal organization as judged from X-ray reflectograms and associated Patterson functions: "no order", no interference peaks detected in reflectograms, except Kiessig fringes associated to film thickness; no regularly spaced significant oscillations detected in Patterson functions; "part. ord.", constructive and/or destructive interference peaks detected in reflectograms, in addition to Kiessig fringes; oscillations detected in Patterson functions, over distances smaller than the film thickness, indicating restricted coherence of the lamellar stacking; repeat distances of the stacking are reported between parentheses; "ordered", similar to previous case, except that the coherence of the stacking extends over the whole film thickness (for the range of probed film thickness); the repeat period is given between parentheses; "not applic.", film did not grow; "−", no data acquired for this pair of polyelectrolytes.

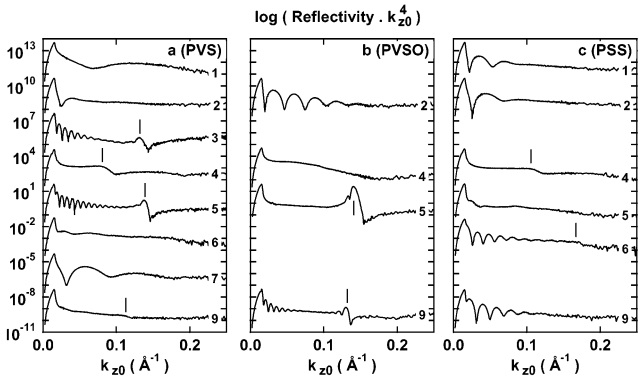

Figure 2. X-ray reflectograms of LBL films grown from **PVS** (a), **PVSO** (b), or **PSS** (c) combined with the different ionenes of this study (identified by the numbers in the figures, with reference to Figure 1). Bragg peaks are indicated by vertical lines. All samples shown were grown for 6 full dipping cycles, except (**3**/**PVS**), (**6**/**PVS**), and (**9**/**PVSO**), which were grown for 7, 16, and 8 dipping cycles, respectively. Curves were displaced vertically by multiplying them by $10^{(24-3n)}$, where n is the number identifying the polycation (except for curves based on polycation **9**, which were not displaced).

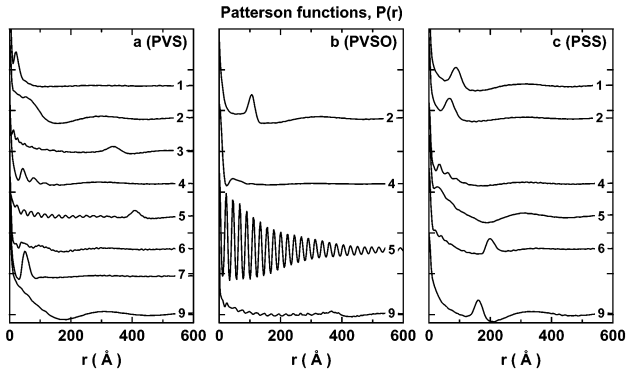

Figure 3. Patterson functions of LBL films grown from **PVS** (a), **PVSO** (b), or **PSS** (c) combined with the different ionenes of this study (identified by the numbers in the figures, with reference to Figure 1). For some samples, regular oscillations in $P(r)$ testify for internal ordering of the multilayers. All samples shown were grown for 6 full dipping cycles, except (**3**/**PVS**), (**6**/**PVS**), and (**9**/**PVSO**), which were grown for 7, 16, and 8 dipping cycles, respectively.

into three categories according to their internal organization: ordered films, into which a lamellar organization extends over the whole film thickness; partially ordered films, into which a lamellar organization only exists over a restricted range of the film, or for which the lamellar organization exists over the whole film thickness but is restricted in coherence to lengths smaller than the film thickness; and unordered films, for which no Bragg peak shows up in the reflectograms, nor oscillations in $P(r)$ (or oscillations are too weak to be ascertained as real). There is some degree of arbitrariness in this classification: Some films also display weak evidences for order, and it is difficult to decide whether they are partially ordered or not ordered; also, for at least partially ordered films, the coherence of the stacking may extend over more or less long distances depending on the details of the fabrication procedure. In addition, the coherence length will always be smaller than film thickness for very thick films. Nevertheless, the classification adopted in this paper may still serve as a useful heuristic tool.

Fully ordered films were only found for some pairs of polyelectrolytes, containing ionenes **5** or **9**. Moreover, partial order was found for some pairs containing polycations **3**−**6** or **9**. However, appearance of (partial) order is subjected to pairing the ionene to specific polyanions (e.g., **9** combined with **PVSO** is fully ordered, only partially ordered when combined with **PVS**, and not ordered at all if paired with **PSS**). Films lacking order were always found for polycations **1**, **2**, and **7** (**8** failing to give rise to films). The values of repeat period were usually found to be unrelated to the value of increment of thickness per dipping cycle, as already observed previously for similar organic[23] and partially ordered hybrid[18,22] multilayers.

To obtain a more complete view of the structure of ordered films, electron density profiles were derived from the reflectivity

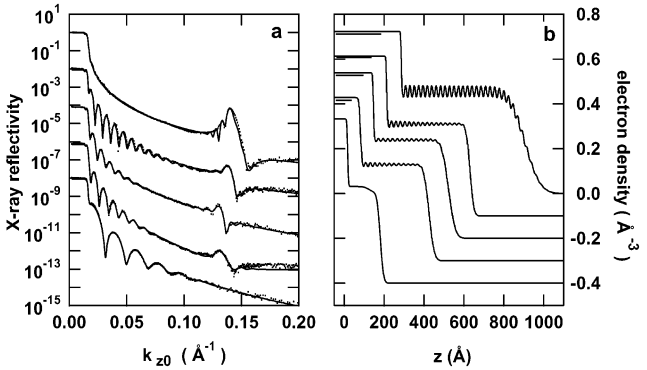

Figure 4. Fits of the X-ray reflectivity of selected samples of this study. Data are plotted as dots, and fits are shown as continuous lines, in (a). The electron density profiles obtained from the fits are shown in (b). From top to bottom: (**5**/**PVSO**)$_6$, (**5**/**PVS**)$_6$, (**9**/**PVSO**)$_8$, (**3**/**PVS**)$_7$, (**9**/**PSS**)$_6$ on silicon. Reflectivities were displaced downward by dividing them by 10^{2n} ($1 < n < 4$), except for the top curve which was not displaced. Electron densities are shifted downward by increments of 0.1 Å^{-3} (a lateral displacement of the density profiles was also applied).

data. Fits and results are presented in Figure 4. For the sake of comparison, a fit was also performed for a typical amorphous film based on **9** and **PSS**. For the ordered samples shown in Figure 4, oscillations can be detected over the whole film thickness. In some instances, oscillations are progressively damped as the distance form the substrate increases, testifying for the existence of a disordering mechanism. In all cases, the number of oscillations is significantly larger than the number of dipping cycles (by a factor of 1.5 to 4), in good agreement with the observations derived from the Patterson functions. The amplitude of oscillations remains small, on the order of a few percents of the average film density, which is expected because electron densities of carbonaceous materials are usually close together. Regions of higher electron density must coincide with layers containing the electron-richer sulfur-bearing polyanions, whereas lower densities are expected for the polycations which contain aliphatic moieties. It is therefore logical to observe that the first layer adsorbed on the silicon is of lower density, testifying for the accumulation of the polycation at this interface.

Discussion

It seems first appropriate to statistically discuss our results. Among the 21 pairs of polyelectrolytes tested, 2 did not give rise to growth, 4 gave rise to nonlinear growth, 4 gave rise to partly linear growth (a case not uncommonly reported in the literature), and 9 gave rise to linear growth. Considering the relatively low linear charge density of the polycations used, at least when compared to the polycations most often encountered in the LBL literature (such as poly(diallyl-dimethylammonium chloride), poly(ethylene imine), poly(allyl-amine hydrochloride), ...), we found that reaching such a high rate of success for the growth of multilayers is very satisfactory. This illustrates once again (if still needed) the remarkable versatility of the LBL technique. The two systems not giving rise to multilayers were found to form soluble complexes upon coprecipitation of the polyelectrolytes, suggesting this may be one of the reasons for the absence of growth. However, it is worthy to note that systems (**1**/**PVS** and **1**/**PSS**) which formed soluble complexes upon coprecipitation could nevertheless be grown as LBL multilayers.

Among the 19 pairs of polyelectrolytes that allow one to grow films, 10 resulted in unordered films, 6 result in partially ordered films, and 3 result in fully ordered films. This indicates that ordered binary organic multilayers may not be so uncommon as initially thought. Of importance here is to note that partial order in multilayers could escape a casual visual inspection of the reflectograms (in this respect, Patterson functions seem to be better suited to detect order). In addition, order appears to require a specific pairing of polycation with polyanion, as it may or may not appear depending on the polyanion selected. Given the limited number of chemical systems tested in the literature, it is thus not surprising that ordered organic multilayers have been essentially overlooked so far.

Second, it is tempting to try to correlate the mode of growth of the multilayers (linear vs nonlinear) with the inner structure of the films. However, mode of growth and organization of the film appear to be almost perfectly uncorrelated. For instance, (**9**/**PVSO**) provides ordered films growing nonlinearly, while (**5**/**PVS**) leads to ordered films growing linearly. Similarly, unordered films may (e.g., **7**/**PVS**) or may not (e.g., **1**/**PSS**) grow linearly. The reader will find many other instances. This lack of correlation is not quite surprising, considering that the values of the repeat period (when any) are most often unrelated to the values of increment of thickness per dipping cycle. This illustrates that growth and structuring of the multilayers are governed by largely independent forces, growth being primarily governed by electrostatics (charge balance) and structuring being governed by mesogenic, hydrophobic, and similar forces. As discussed more completely elsewhere,[23] electrostatics governs the amounts adsorbed at each cycle (although other forces may also play a secondary role, as demonstrated by others[43]); organization of this adsorbed layer will occur independently. This explains why the number of oscillation periods in the films is much larger than the number of dipping cycles used to prepare the sample (Figure 4).

Third, one may wonder whether there is an equivalence between the structure of bulk complexes obtained by coprecipitation and the structure of films grown by LBL deposition. Maybe surprisingly, the answer is rarely positive. For instance, four pairs for which LBL films display evidences for layering (**4**/**PVS**, **6**/**PSS**, **9**/**PVS**, **9**/**PVSO**) fail to provide evidence for ordering in bulk complexes. Conversely, one pair (**4**/**PVSO**) forms ordered bulk complexes but amorphous LBL films. Finally, when both films and bulk complexes show evidence for ordering, repeat periods are often similar (**4**/**PSS**, **5**/**PVS**, **5**/**PVSO**), but not always (**3**/**PVS**). These differences are obviously due to differences in sample preparation: Bulk complexes are obtained through a rapid precipitation from solution, while complexes in ESA films grow in conditions closer to equilibrium while feeling the two-dimensional force field of the substrate. On the positive side, this suggests that ordering may be enhanced by specific processing conditions.

Fourth, it is possible to correlate the internal structure of the multilayers with the chemical architecture of the polycations. Among all of the systems tested, fully ordered films were only obtained with ionenes giving rise to lyotropic mesophases (i.e., liquid crystallinity in water); partially ordered films were also obtained with ionenes not giving rise to lyotropic mesophases but bearing a 4-(4′-nitrophenylazo)-phenyl strongly mesogenic

(43) Büscher, K.; Graf, K.; Ahrens, H.; Helm, C. A. *Langmuir* **2002**, *18*, 3585.

side group or a $-C_{10}H_{20}-$ segment. Conversely, order was *never* observed in ESA films grown from ionenes not bearing these moieties. It may thus be concluded that the presence of structure-forming groups such as long hydrophobic segments (prone to microphase separation in water) or strong mesogenic side groups is required to obtain at least partially ordered films. This is a required but not a sufficient condition, as order may or may not appear depending on the polyanion used. The propensity to form internally structured multilayers is thus directly related to the trend of the ionene to form some structure in water; however, the relationship is not univocal, being also controlled by the specific matching between the polyanion and the ionene considered. This nonunivocal relationship may explain why a number of studies by others[44−46] on LBL films grown from liquid crystalline polymers did not reveal the presence of Bragg peaks in X-ray reflectograms.

These observations provide support to the notion that ordered multilayers result from prestructuring of the ionene in the water-swollen layer adsorbed at the surface of the film; subsequent penetration of this layer by the polyanion will result either in destructuring and formation of films of amorphous complexes or in the formation of an organized complex giving rise under certain circumstances to highly ordered multilayers. Depending on the amounts adsorbed (increment of thickness per dipping cycle), the structuring process will give rise to a given number of repeat periods per dipping cycle. On the basis of an in-depth study of the **5**/**PVS** system, we have recently discussed the growth and pathway to structuring of such multilayers.[23] This needs not be repeated here. However, it is important to emphasize that the observed difference between the increments of thickness per dipping cycle and the internal repeat periods of the films indicates that there is no direct, one-to-one, correspondence between film structure and sequence of deposition. In this respect, the main interest of such internally organized films lies essentially in the possibility of aligning and confining spatially specific functional groups, rather than in obtaining a structure for which the internal layering would reflect exactly a given sequence of dipping cycles. For the latter requirement, alternative methods such as Langmuir−Blodgett films seem more appropriate.[47]

Finally, it is appropriate to make a few comments on the very notion of order and layering, in relation with the technique used to probe it. X-ray reflectivity is effectively sensitive to the electron density profile, laterally averaged over the coherence area of the photons.[48,49] Bragg peaks will thus only be observed when layers can be defined over this area (on the order of 1 μm^2 for our setup). If the lateral extension of the layers is much smaller, and if the vertical positions of such layers in neighboring areas are not related to each other by a fixed relationship, Bragg peaks will tend to vanish. Nevertheless, close to the substrate, true layering should still occur, due to the constraints posed by the impenetrable wall of the substrate. This is very similar to the case of hybrid multilayers based on the random tiling of small clay platelets, which we have discussed extensively elsewhere.[22d] A broad Bragg peak should then be detectable in the reflectograms, and Patterson functions should display a few oscillations close to the origin. This is indeed what can be observed for some of our samples, which were grouped under the denomination "partial order". Even for ordered samples, partial damping of the density fluctuations can be seen (Figure 4), indicating that the layering becomes less defined as the distance from the substrate increases. A more complete study could thus involve a determination of the lateral extent of the layering, by using X-ray diffuse scattering, for example, and relating it to the degree of vertical order as judged from X-ray reflectivity. This is, however, outside of the scope of the present study. Finally, any type of ordering not giving rise to fluctuations of electron density in the vertical direction will largely escape detection by XRR. It may thus be that some order exists in the films in the lateral direction, although this is not very probable and would be of restricted practical significance.

Conclusions

We have systematically studied the growth and internal structure of multilayers obtained by combining, in turn, nine ionenes with three polyanions. Contrary to a general belief, ordered organic binary multilayers are by no way exceptional, provided one of the polyelectrolytes bears groups tending to induce structure in water, such as long hydrophobic segments or strong mesogens. In this respect, systems capable of forming lyotropic mesophases are conducive to multilayers of higher order. However, this condition is not sufficient, as order will or will not emerge in the multilayer depending on the pairing of the ionene with specific polyanions. These results suggest that order in the multilayer results from some degree of prestructuring of the water-swollen layer adsorbed during each step of deposition. Other outcomes of this study are the often-observed difference of structure between complexes in multilayers and bulk complexes, and the complete decorrelation between mode of growth (linear or not) and internal structure of the multilayers. This is in good agreement with the observed independence of increments of thickness per deposition cycles and internal repeat periods of the multilayers. Possible uses of such ordered multilayers are to be found in applications where preferential alignment of specific functional groups is required, or when strong confinement of such functions is desirable.

Acknowledgment. We thank Bernd Mayer for the preparation of some of the ionenes used in this work, and Patrick Bertrand and Arnaud Delcorte for helpful discussions. Financial support was provided by the DG Recherche Scientifique de la Communauté Française de Belgique (Actions de Recherches Concertées, conventions 94/99-173 and 00/05-261) and by the Belgian National Fund for Scientific Research.

JA0283807

(44) Cochin, D.; Passmann, M.; Wilbert, G.; Zentel, R.; Wischerhoff, E.; Laschewsky, A. *Macromolecules* **1997**, *30*, 4775.
(45) Passmann, M.; Wilbert, G.; Cochin, D.; Zentel, R. *Macromol. Chem. Phys.* **1998**, *199*, 179.
(46) Passmann, M.; Zentel, R. *Macromol. Chem. Phys.* **2002**, *203*, 363.
(47) Petty, M. C. *Langmuir−Blodgett Films: An Introduction*; Cambridge University Press: Cambridge, 1996.
(48) Tolan, M. *X-ray Scattering from Soft-Matter Thin Films*; Springer: Berlin, 1999.
(49) Daillant, J.; Gibaud, A. *X-ray and Neutron Reflectivity: Principles and Applications*; Springer: Berlin, 1999.